Journal of the Nigerian Association of Mathematical Physics
Volume **20 (March, 2012), pp 315 – 320**

Evaluation of Fractured Basement Complex Rock Porosity by Azimuthal Cross-Square Vertical Electrical Soundings

[1]Saleh M., [2]Likkason O. K. & [3]Mohammed Hassan

[1]Department of Physics, Bayero University, Kano, Nigeria
[2]Physics Programme, ATBU, Bauchi, Nigeria
[3]Department of civil Engineering, University of Maiduguri, Nigeria

Abstract

This paper gave an overview on the use of Azimuthal Cross-Square direct-current resistivity sounding as complementary geophysical technique to Schlumberger vertical electrical sounding in characterizing fractured geologic systems. Previously, Schlumberger vertical electrical sounding was used to collect data. Interpretation of the generated data revealed the stratigraphic setting and identified anomalous feature at the downstream section of Tiga Dam, Northwestern Nigeria. The feature was large in size, appeared deep down and at an angle to the extended tip of the locality surface manifested fractures and increase in size on approaching the core of the dam. These prompted the use of Azimuthal Cross-Square Array direct-current resistivity soundings about eight strategically selected points in order to characterize the fractures and the anomalous feature. Some of the parameters deduced were depth of fracturing (76.00m – 126.02m), anisotropy (1.02 – 1.43), fracture swarthiness and secondary porosity (0.01 – 0.28). Specifically the anomalous body has porosity ranging from 0.16 to 0.28.

Keyword: Anomalous, Azimuthal, Foliation, Porosity and Swarthiness.

1.0 Introduction

The study was embarked with sole aim of characterizing the surface manifested lineaments. An earlier work based on direct-current vertical electrical soundings (VES) using Schlumberger array showed that the lineaments appeared to have extended deep down and in addition detected the presence of an anomalous feature [1]. The work was conducted at the downstream of the Tiga dam. The earth work at the dam was down to a depth of 13m below riverbed with embankment of height 48m above. The feature appeared far below the embankment and appeared to grow in size on approaching the core. The feature was later interpreted to be a fracture in an environment (Basement complex) that its competence to support the present structure was not in any way doubted at the time of establishing such mighty structure and its accompaniment. But the identification and characterization of fractures is important in rocks with low primary (or matrix) porosity because the bulk porosity and permeability are determined mainly by the intensity, orientation, connectivity, aperture, and infill of fracture systems [2] and fracture serves as weak zone that could easily yield to excessive stress. Moreover, once initiated, fractures themselves significantly alter the stress field in adjacent rock. In an effort to characterize the fracture, Azimuthal Cross-Square Resistivity Soundings (ARS) were used to determine the porosity of the identified fractures. The ARS were conducted about eight preselected points about the fractures based on the earlier work [1].When compared, the Schlumberger array has the disadvantage of low signal-to-noise ratio and the depth of investigation is nearly one-third of the maximum electrodes spacing [3]. This means that depth of penetration is low. Nevertheless, it supersedes other collinear arrays in stratigraphic studies ([3];[4]and[5]).Whereas the cross-square array has the advantages of being volumetric sampler and high depth of penetration. Depth of investigation is equal to separation between the electrodes ([6], [7] and [8]). The non-collinear arrays are about twice more sensitive to anisotropy as are collinear arrays; most prominent [among the non-collinear] is square-array [9].

[1]Corresponding author: ***Saleh M.,*** E-mail: muhmusabi@yahoo.co.uk, Tel. +2348069289985

2.0 Theory and Methodology

The apparent resistivity ρ_a of a given layer traversed by current is given by

$$\rho = \frac{\Delta V}{I} K \quad \text{……..(1)}$$

Where $V_1 - V_2 = \Delta V$ is the measured potential difference, I the injected current and K the geometrical factor. For cross-square array (Figure 1) the expression for K is

$$K = \frac{2\pi A}{2 - \sqrt{2}} \quad \text{……..(2)}$$

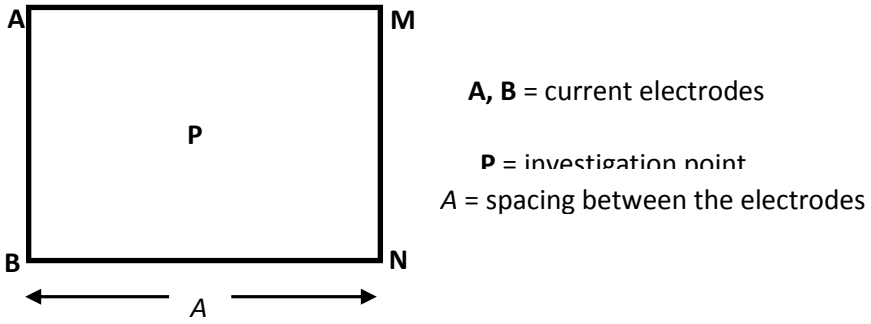

Figure 1: Cross-Square Array

The values of apparent resistivity are affected by the location and spacing of electrode array, the larger the spacing, the sample volume (sample depth). In addition, if the electrical properties of the region vary with direction (anisotropic), the apparent resistivity can also be dependent on the azimuth of the array. The plane of anisotropy is generally parallel to the surface for horizontally stratified rock. In vertically fractured rock units, the plane is not parallel to the surface, and the measured apparent resistivity will be dependent on array orientation. For each square, three measurements are made: two perpendicular measurements (alpha, α ; and beta, β) and one diagonal measurement (gamma, γ) (Figure 2). When the current electrodes are put on the side of the square aligned perpendicular to an azimuth, the resistivity value of that setup is called the alpha-resistivity (ρ_α). When the current electrodes are on the side of the square along an azimuth the resistivity is called the beta-resistivity (ρ_β). The α and β measurements provide information on the directional variation of the subsurface apparent resistivity ρ_a . The azimuthal orientation of the α and β measurements is that of the line connecting the current electrodes. The γ measurement serves as a means of checking the level of anisotropy. Busby and Peart [10] have explained that the measured value of γ is zero or about that only when the volume of rock investigated is not sufficient (because the electrode array spacing is too small) for the rock to behave anisotropically or there is no measurable fracture.

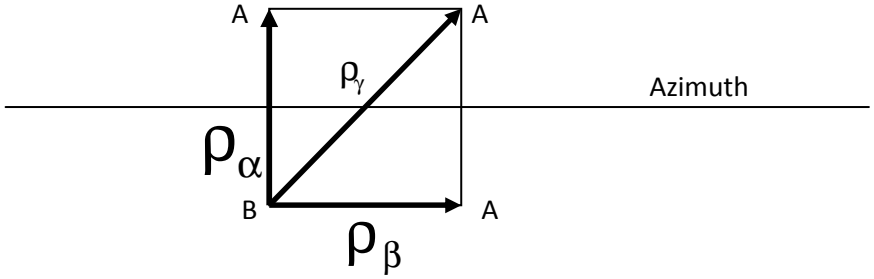

Figure 2: Orientation of Current Electrodes and Corresponding Resistivity Parameters

The array was rotated in 30° increments from 0° to 180°. The 0° azimuth was regarded as the reference azimuth and was oriented in the N-E direction. At each angle, data from multiple size squares were collected to image different depths. The measurement was conducted, about 8 preselected investigation points (Table 1), in similar manner to collinear, yielding resistivity values in 6 different directions. The array was expanded symmetrically about the center point, in increments of $A(2)^{½}$ in accordance with [6] approach, so that the data can be interpreted as a function of depth (sounding). The A values used were 5, 7, 10, 14, 20, 28, 40, 72, 100 and 140m depending on peculiarity of investigation point. This provided an opportunity for making comparison with the VES results and yielded a total of about 120 resistivity readings per each investigation point.

Table 1: Metadata for the ARS Investigation Points

Invest. Point	Lat. (North)	Long. (East)	Elev. (m)	Description of Points in relation to First Phase Equivalent geologic sections
1	$11^0 27' 54.3"$	$8^0 24' 34.5"$	498	At profile 1 on VES point 13
2	$11^0 27' 54.3"$	$8^0 24' 34.9"$	497	At profile 2 on VES point 9
3	$11^0 27' 54.8"$	$8^0 24' 33.1"$	491	At profile 2 on VES point 13
4	$11^0 29' 00.9"$	$8^0 24' 40.0"$	502	At profile 1 on VES point 3
5	$11^0 27' 54.6"$	$8^0 24' 33.8"$	498	At profile 1 on VES point 6
6	$11^0 27' 54.3"$	$8^0 24' 31.6"$	498	At profile 1 on VES point 1
7	$11^0 27' 56.5"$	$8^0 24' 34.3"$	496	At profile 2 on VES point 7
8	$11^0 27' 57.0"$	$8^0 24' 35.4"$	495	At profile 2 on VES point 3

3.0 Data Analysis And Interpretation

The ARS graphical technique developed by [6] was used to determine porosity of the fractures. For a zone of oriented, saturated steeply dipping fractures, the ARS data have an apparent resistivity minimum oriented in the same direction as the dominant fracture direction (strike).

The data for each A-spacing was plotted graphically about corresponding azimuth for particular A-spacing. Each graphical display was mirrored on polar coordinates to yield 360 degrees plot (Figures 3 and 4) in a computer program trademarked Origin (version 5.0) developed by Microcal Software Inc, USA.

For a homogenous anisotropic medium, the coefficient of anisotropy, λ, generally ranges between 1 and 2 [5]. This provided a useful criterion for smoothing the raw-data plots using Fast Fourier Transform (Figures 3 and 4). Lane, Haeni and Watson [11] have recommended the use of interpretative method of [7] as a useful tool for studying the variations in azimuthal resistivity caused by fractures and defined the principal fracture strike direction as being perpendicular to the direction of maximum resistivity. In line with Lane's [11] idea, the principal/dominant fracture strike was identified for each A-Spacing plot and the stacked up polar plots.

Habberjam [7] has shown that secondary (fracture) porosity Φ can be estimated as

$$\Phi = 3.41 \times 10^4 \frac{(\lambda-1)(\lambda^2-1)}{\lambda^2 C(\rho_{max}-\rho_{min})} \quad (1)$$

. Where ρ_{max} is maximum resistivity value on a polar plot and ρ_{min} is the corresponding minimum resistivity value on the plot at specified depth (Table 2), C is the specific conductance of groundwater in microsiemens per centimetre, estimated to be 131.5 microsiemens per centimetre for underground water from the area obtained from the work of [12] and λ is the coefficient of anisotropy. However, according to [5], the coefficient of anisotropy for square array can be defined as the square root of ratio of apparent resistivity measured perpendicular to a fracture strike to apparent resistivity parallel to the fracture strike. These are the maximum and minimum apparent resistivities given in the Habberjam [7] porosity expression. Therefore, the coefficient of anisotropy λ can by re-expressed as

$$\lambda = \sqrt{(\frac{\rho_{max}}{\rho_{min}})} \quad (2)$$

The principal fracture strike angle, $\rho_{max}$and ρ_{min}values were determined from the individual polar plots and used to calculate the λ and Φ using equations (1) and (2). The values are given in Table 2. Typical demonstration for

calculating the values of the variables in Tables 2 are shown below.

Consider point 1 polar alpha-plot for A=5m (Figure 3). The deduced ρ_{min} is the mean value of the interpolated values on the extreme sides of the minor axis on the Fast Fourier Transform (FFT) smoothed ellipse and is 75.76 Ωm, whereas ρ_{max} is the mean value interpolated on the extreme sides of the major axis on the FFT smoothed ellipse and is 109.06Ωm. From

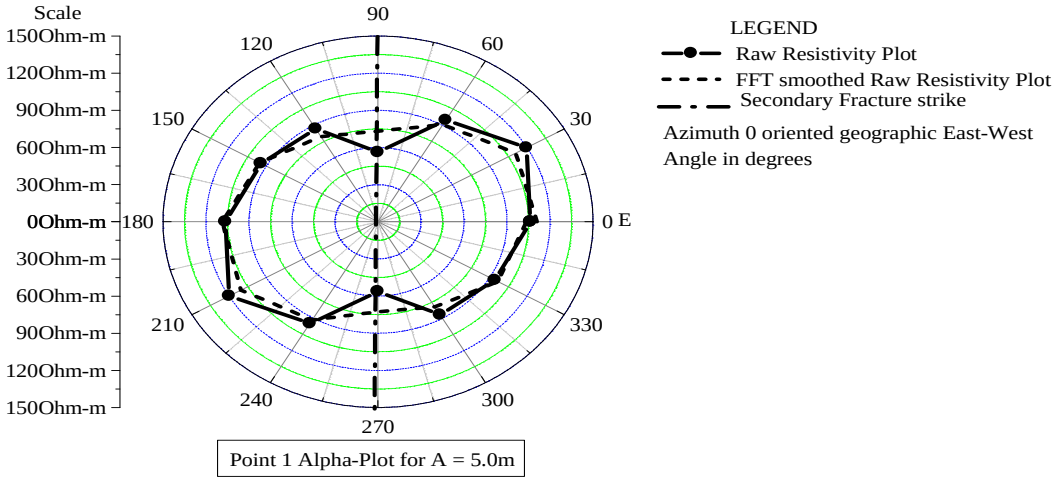

Figure 3: Point 1 Polar Alpha-Plot for A = 5.0m

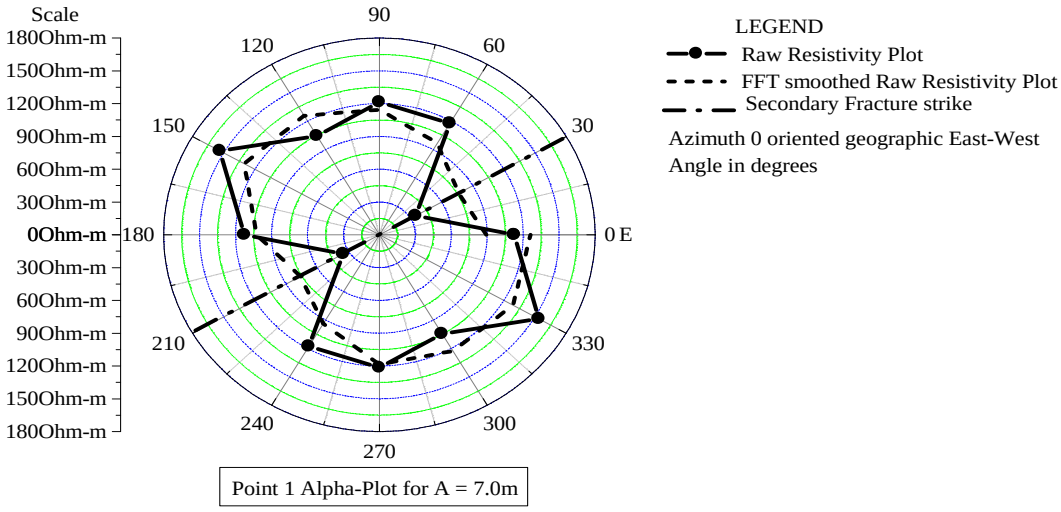

Figure 4: Point 1 Polar Alpha-Plot for A = 7.0m

equation (2), the value of λ at a depth of 5.0m could be calculated based on these deduced values as

$$\lambda = \sqrt{\frac{109.06}{75.76}} = 1.02 \qquad (3)$$

From equation (1), the value of Φ at the same depth was calculated as follows

$$\Phi = 3.41 \times 10^4 \frac{(1.02-1)((1.02)^2-1)}{(1.02)^2 C(109.06-75.76)} = 0.12 \qquad (4)$$

The values of the interpolated and calculated parameters are placed in the first row of Table 2.

The same procedure is applied to polar plot at depth A = 7.0 m (Figure 4). The values of the interpolated parameters were for $\rho_{min} = 78.07$ Ωm and $\rho_{max} = 126.10$ Ωm. Thus, the value of λ at this depth would be 1.27 leading to the value of Φ as 0.16. These values are shown in the second row of Table 2.

4.0 Discussion

Looking at Table 2, the fracture strike direction which is synonymous with the fracture foliation direction, ∅, referenced to zero azimuth could be deduced. The zero azimuth is regarded as the geographic N-E direction and coincides with the direction of orientation of the profiles in the field. As can be seen in Figures 3 and 4, the fracture strike angle (the direction for ρ_{min} measured anticlockwise) for depth A=5.0m at ARS point 1 was $\emptyset = 90^0$ from the zero azimuth, while the fracture strike angle for depth A=7.0m is $\emptyset = 30^0$from the reference azimuth. The same procedure was used to generate the rest of the rows for the different investigation depths in Table 2. The Alpha and Beta columns for the tables correspond respectively to the values of interpolated and calculated parameters when the ARS array was oriented at 90^0 from each other. The values of fracture strikes directions for the two ARS array orientations showed slight violation of the principle of reversibility of current flow lines. Even though the two arrays were oriented 90^0 apart, the corresponding fracture strike directions at certain depths differ by $60^0$and not 90^0 as expected. The values observed to occur at depths with appreciable porosity values was 30^0. These depths were the locations of crossing fractures. However at depths where porosity values are low the fracture strike direction was between 30^0 and 90^0.

Table 2: Electrical Parameters for ARS First Point

		Alpha						Beta					
S/N	A(m)	ρ_{max} (Ωm)	ρ_{min} (Ωm)	ρ_m **(Ωm)**	λ	Φ	∅ (°)	ρ_{max} (Ωm)	ρ_{min} (Ωm)	ρ_m (Ωm)	λ	Φ	∅ (°)
1	5	109.06	75.76	90.90	1.20	0.12	90	110.11	76.73	91.92	1.20	0.12	30
2	7	126.10	78.07	99.22	1.27	0.16	30	178.47	130.76	152.76	1.17	0.10	0
3	10	285.71	182.00	228.03	1.25	0.15	0	190.78	139.19	162.96	1.17	0.10	90
4	14	266.40	189.03	224.40	1.19	0.11	150	228.85	188.77	207.85	1.10	0.06	60
5	20	467.67	236.00	332.22	1.41	0.26	150	388.36	218.01	290.97	1.33	0.21	90
6	28	346.48	175.31	246.46	1.41	0.26	30	481.18	252.56	348.61	1.38	0.24	90
7	40	420.11	261.51	331.46	1.27	0.16	90	445.02	239.68	326.59	1.36	0.23	30
8	50	505.50	365.20	429.66	1.18	0.10	90	430.10	250.36	328.15	1.31	0.19	30
9	72	800.00	415.67	576.66	1.39	0.25	0, 90	775.42	500.10	622.73	1.25	0.15	30,120
10	100	539.14	416.07	473.62	1.14	0.08	90	485.90	306.45	385.88	1.26	0.16	30
11	140	1327.80	1327.80	1327.80	1.00	0.00	xxx	1282.51	1282.51	1282.51	1.00	0.00	xxx
		Inferred depth to bottom of the fracture = 126.02m											
		Fracture swath angle in degrees = 30											
		Oblique fracture angle in degrees = 0, Main Fracture angle in degrees = 90											

Looking at Table 2, we note two inferred fractures: one oriented at $\emptyset = 0^0$ and the other at $\emptyset = 90^0$ for Φ = 0.25. The computed value of Φ = 0.25 showed that the region is sufficiently porous. The $\emptyset = 90^0$ coincides with surface manifested fracture direction, hence it is regarded as continuation of surface fracture. The value $\emptyset = 0^0$ was presumed to be an oblique fracture coming from the core of the dam. The $\rho_{min} = 576.66$ Ωm coupled with Φ = 0.25 (the highest value of porosity occurring only at this depth) could be regarded as a resistivity of a region invaded by fluid (water) disturbed by the effect of un-fractured region, as ARS array is a volumetric sampler. Consequently, the presence of a

unique oblique fracture with $\emptyset = 0^0$ with porosity value and when combined with the moderate resistivity values, the region can generally be thought as having an oblique fracture at depth of 72.0m coming from the core of the dam. This is similarly true in respects of other ARS points. The location with distinctive parameters can be identified at depth between 50m to 72m within the ARS plot value and approximate porosity of 0.25 in addition of having dual peaks. The two peaks represent two fractures. The one oriented at $\emptyset = 90^0$ to the reference azimuth was regarded as continuation of surface manifested fracture whereas the other was taken to be the oblique fracture.

5.0 Conclusion

The values of calculated porosity at various depths traversed by current in combination of other parameters could be used to have in depth understanding of fractured formation. This information proved very useful as formation strength (competence) to support overburden created by human artifacts is largely dependent on such properties of rock bordering on its consolidation, permeability, turtosity and degree of fracturing. Moreover, the ability to transmit fluid in formation is closely related to these properties, thereby making this approach a very useful tool in the study of migration of contaminant, aquifer detection and characterization.

References

[1] Saleh, M and Likkason, O. K., 2011, Geoelectric Appraisal of Lithostratigraphic Features of Downstream of the Tiga Dam, NW Nigeria, Journal of National Institute of Physics, vol 22, No. 1, p29-37.

[2] Skjernaa, L., and Jørgensen,N.O., (1993), Detection of local fracture systems by azimuthal resistivity surveys: examples from south Norway: Memoirs of the 24th Congress of Internat. Assn. Hydrogeologists, 662–671.

[3] Zohdy, A. A. R., (1989). A new method for the automatic interpretation of Schlumberger and Wenner sounding curves, Geophysics 54(2), 245-253.

[4] Telford, W.M., Geldart, L.P., and Sheriff, R.E., (1990), Applied geophysics (4th ed.): New York, Cambridge University Press.

[5] Keller, G.V., and Frischknecht, F.C., (1966), Electrical methods in geophysical prospecting: London, Pergamon Press.

[6] Habberjam, G.M., and Watkins, G.E., (1967), The use of a square configuration in resistivity prospecting: Geophysical Prospecting, v. 15, p. 221-235.

[7] Habberjam, G.M., (1972), The effects of anisotropy on square array resistivity measurements: Geophysical Prospecting, v. 20, p. 249-266.

[8] Habberjam, G.M., (1979), Apparent resistivity, anisotropy, and strike measurements, Geophysical Prospecting, v. 23, p. 211-247.

[9] Taylor,R.W., and Fleming,A. H., (1988), Characterising jointed systems by azimuthal resistivity surveys: GroundWater, 26, 464–474.

[10] Busby, J. P. and Peart, R. J. (2007), Azimuthal Resistivity and Seismic Measurements for the Determination of Fracture Orientations, Regional Geology Group, British Geological Survey, Keyworth, Nottingham, NG1256G, United Kingdom.

[11] Lane, J. W., Haeni, F. P., and Watson, W. M., (1995). Use of Square Array Direct-Current Resistivity Methods to Detect Fractures in Crystalline Bedrock in Hampshire.Groundwater , 20 (3), 476-485.

[12] Kabir, M. (2008), Laboratory Method of Measuring Electrical Properties of Earth Materials around Tiga Dam, Kano State, Northwestern Nigeria, Unpublished B. Sc. Thesis, Department of Physics, Bayero University, Kano, Nigeria.